HHS Public Access

Author manuscript

ACS Appl Bio Mater. Author manuscript; available in PMC 2024 December 16.

Published in final edited form as:

ACS Appl Bio Mater. 2024 November 18; 7(11): 7675–7683. doi:10.1021/acsabm.4c01239.

A Self-Amplifying Human Papillomavirus 16 Vaccine Candidate Delivered by Tobacco Mosaic Virus-Like Particles

Sweta Karan,

Aiiso Yufeng Li Family Department of Chemical and Nanoengineering, University of California, San Diego, La Jolla, California 92093, United States; Shu and K. C. Chien and Peter Farrell Collaboratory and Center for Nano Immuno Engineering, University of California, San Diego, La Jolla, California 92093, United States

Jessica Fernanda Affonso De Oliveira,

Aiiso Yufeng Li Family Department of Chemical and Nanoengineering, University of California, San Diego, La Jolla, California 92093, United States; Shu and K. C. Chien and Peter Farrell Collaboratory and Center for Nano Immuno Engineering, University of California, San Diego, La Jolla, California 92093, United States

Miguel A. Moreno-Gonzalez,

Aiiso Yufeng Li Family Department of Chemical and Nanoengineering, University of California, San Diego, La Jolla, California 92093, United States; Shu and K. C. Chien and Peter Farrell Collaboratory and Center for Nano Immuno Engineering, University of California, San Diego, La Jolla, California 92093, United States

Nicole F. Steinmetz

Aiiso Yufeng Li Family Department of Chemical and Nanoengineering, University of California, San Diego, La Jolla, California 92093, United States; Shu and K. C. Chien and Peter Farrell Collaboratory, Center for Nano Immuno Engineering, Department of Bioengineering, Department of Radiology, Institute for Materials Discovery and Design, Moores Cancer Center, and Center for Engineering in Cancer, Institute of Engineering Medicine, University of California, San Diego, La Jolla, California 92093, United States

Corresponding Author: Nicole F. Steinmetz – Aiiso Yufeng Li Family Department of Chemical and Nanoengineering, University of California, San Diego, La Jolla, California 92093, United States; Shu and K. C. Chien and Peter Farrell Collaboratory, Center for Nano Immuno Engineering, Department of Bioengineering, Department of Radiology, Institute for Materials Discovery and Design, Moores Cancer Center, and Center for Engineering in Cancer, Institute of Engineering Medicine, University of California, San Diego, La Jolla, California 92093, United States; nsteinmetz@ucsd.edu.

Author Contributions

All authors contributed to the writing of this manuscript and approved the final version. S.K.: mRNA design, development and characterization of TMV.Nod.HPVE7.OAS, *in vitro* expression, testing humoral immunity in mice, data analysis and figures, and draft and revision of manuscript. J.F.A.D.O.: collection of blood, splenocyte assay, and revision of manuscript. M.A.M.-G.: splenocyte assay and revision of manuscript. N.F.S.: conceptualization, funding acquisition, project management, data analysis, and draft manuscript and revisions.

Supporting Information

The Supporting Information is available free of charge at https://pubs.acs.org/doi/10.1021/acsabm.4c01239.
Shuffled E7-Nodamura sequence, schematic representation of the Nod.HPVE7.OAS mRNA construct, and *in vitro* transcribed Nod.HPVE7OAS mRNA (PDF)

Complete contact information is available at: https://pubs.acs.org/10.1021/acsabm.4c01239

The authors declare the following competing financial interest(s): Dr. Steinmetz is a cofounder of and has equity in Mosaic ImmunoEngineering Inc. Dr. Steinmetz is a cofounder and manager of Pokometz Scientific LLC, under which she is a paid consultant to Flagship Labs 95 Inc. and Arana Biosciences Inc. Dr. Steinmetz is a cofounder and CEO of PlantiosX Inc.

Abstract

Virus-like particles (VLPs) are naturally occurring delivery platforms with potential for mRNA vaccines that can be used as an alternative to lipid nanoparticles. Here we describe a self-amplifying mRNA vaccine based on tobacco mosaic virus (TMV) expressing a mutated E7 protein from human papillomavirus 16 (HPV16). E7 is an early gene that plays a central role in viral replication and the oncogenic transformation of host cells, but nononcogenic mutant E7 proteins can suppress this activity. Immunization studies involving the delivery of self-amplifying mutant E7 mRNA packaged with TMV coat proteins confirmed the elicitation of E7-specific IgG antibodies. Additional *in vitro* splenocyte proliferation and cytokine profiling assays indicated the activation of humoral and cellular immune responses. We conclude that TMV particles are suitable for the delivery of mRNA vaccines and can preserve their integrity and functionality *in vitro* and *in vivo*.

Graphical Abstract

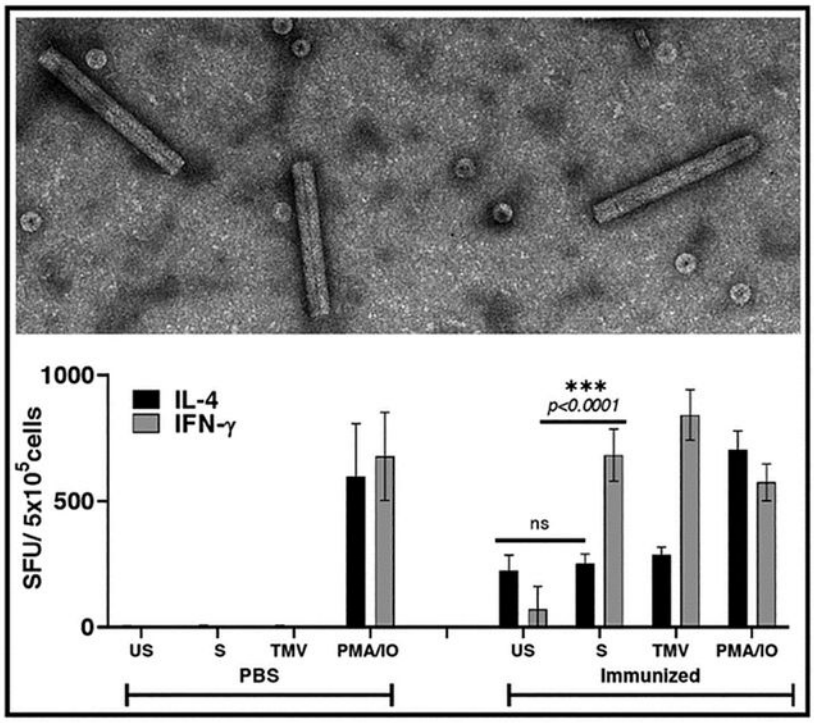

Keywords

virus-like particles (VLPs); tobacco mosaic virus (TMV); self-amplifying mRNA vaccine; E7 oncogene; human papillomavirus 16 (HPV16)

INTRODUCTION

Traditional vaccines are based on the direct introduction of antigens that stimulate an immune response, whereas mRNA vaccines package a translatable RNA molecule encoding the antigen, which is expressed once the mRNA has been taken up by cells.[1] Although

mRNA vaccines have a history stretching back more than 40 years,[1] they have recently gained more attention due to their widespread use during the COVID-19 pandemic.[2] However, they have been developed for a range of indications beyond infectious diseases, including immunotherapy, genetic disorders, regenerative medicine, and cancer.[3–5] The main benefits of mRNA vaccines include the universal design principles, scalability for mass production, safe translation without the risk of genomic integration, and the ability to generate a robust immune response due to the capacity of single mRNA molecules to produce many protein antigens.[3,6] Conversely, the reactogenicity of mRNA vaccines is no different to that of conventional, protein-based counterparts.[7] One key challenge with the delivery of mRNA vaccines is that naked mRNA degrades rapidly *in vivo*. This has been addressed by the development of lipid nanoparticles (LNPs) for mRNA protection and targeted delivery to immune cells.[8] More recently, virus-like particles (VLPs), which resemble the structure of a natural virion but lack the endogenous genome, have been developed as delivery vehicles for drugs and nucleic acids, particularly in the field of immunotherapy, and have also been considered for the delivery of mRNA vaccines.[9–11]

Tobacco mosaic virus (TMV) is a naturally occurring plant virus that has been repurposed to develop a range of VLPs as noninfectious nanomaterials for medical applications.[12] The rod-shaped virion of wild-type TMV is 300 nm in length and 18 nm in diameter, with a central channel of 4 nm.[13] The genomic RNA intercalates with coat proteins and self-assembles into a virion with helical symmetry. However, TMV coat proteins will assemble with any RNA molecules that contain the appropriate packaging sequence, known as the origin of assembly sequence (OAS),[14] forming particles longer or shorter than the wild-type virion according to the size of the RNA. This provides a versatile tool for the construction and delivery of mRNA vaccines. For example, TMV has been shown to package the self-amplifying Nodamura replicon, allowing the expression of functional mRNAs encoding reporters such as luciferase and derivatives of green fluorescent protein *in vitro* and *in vivo*.[10,15] It can also package other viral genomes when endowed with the correct packaging signal, including Semliki Forest virus and ebolaviruses.[10,16–18]

In the context of mRNA vaccine development, TMV is particularly useful because the capsid is extremely robust, conferring stability against extreme temperature and pH, as well as various harsh solvents, allowing distribution without a cold chain.[19] This may be an advantage compared to the LNP technology, because some LNP-based mRNA vaccines, require storage and distribution in ultralow freezers therefore restricting distribution in low-income countries.[20] Further, plant virus large-scale production is inexpensive and straightforward because the coat protein can be produced in massive quantities by molecular farming in plants before mixing with synthetic RNA or RNA produced by *in vitro* transcription.[21] While *in vitro* assembly offers a plug-and-play technology, opportunity exists to produce and self-assemble the vaccine candidate in plants, which may allow to streamline production in the region-for the region and could make a contribution to less resourced areas of the world.[22] As native TMV virions contain a 6-kb genomic RNA,[13] TMV VLPs can encapsulate higher molecular weight RNA cargoes with ease; in stark contrast, encapsulation of longer mRNAs (3–5 kb or above) has been proven challenging with the LNP technology.[4] Finally, TMV-based nanoparticles interact directly with antigen-presenting cells and are transported to the draining lymph nodes.[23] They also function as

pathogen-associated molecular patterns, triggering the innate immune system via pattern recognition receptors.[24–26] TMV VLPs thus exhibit potent adjuvant properties, comparable to the LNPs (the latter often are engineered with immunomodulatory agents).[23] These advantages make TMV an excellent candidate for the development of mRNA vaccines against human papillomaviruses.

Human papillomavirus 16 (HPV16) is associated with a high risk of cancer, including benign and malignant lesions.[27] This nonenveloped virus contains a double-stranded DNA genome of ~8 kb and primarily shows tropism for mucosal and cutaneous epithelia of the genital and upper respiratory tracts, and skin.[28] HPV16 expresses six early genes (E1, E2, E4, E5, E6, and E7) and two late genes (L1 and L2).[29,30] The E6 and E7 are key oncogenic drivers of cervical carcinogenesis, transforming normal cells into cancerous ones by forming complexes with, and thus inactivating, the tumor suppressor proteins p53 (targeted by E6) and pRb (targeted by E7), respectively.[31–33] Both oncogenes are constitutively expressed throughout the HPV life cycle, making them crucial targets for therapeutic vaccine development. Mutations in E6 or E7 suppress their transforming functions in a dominant manner, so the delivery of mRNA encoding the suppressor mutant forms of E6 or E7 can prevent oncogenic transformation.[32] Preclinical and clinical studies of HPV16/18 E6/E7-based vaccines have demonstrated efficacy in treating advanced-stage cervical cancers.[32]

In this proof-of-concept study we only focused on E7. This was to avoid complexity of incorporating two oncogenic antigens with distinct properties into a single mRNA construct. While E6 encodes a larger protein of 150–160 amino acids, with a molecular weight of around 18 kDa,[34] E7 oncogene encodes a relatively small phosphoprotein of about 100 amino acids (~11 kDa). With the concepts established and validated, future work will focus on a dual E7 and E6 vaccine construct.

METHODS

Plasmid Construct.

To express a modified HPV16 E7 protein with limited oncogenic potential, we constructed a self-amplifying Nodamura replicon (Nod) plasmid, pT7.Nod.E7OAS. Synthetic constructs corresponding to the HPV16 E7 protein (GenBank AF536180.1) were prepared by GenScript with mutations in the conserved pRb-binding domain and cysteine repeat region (D21G, C24G, E26G, C61G, and C94G) to suppress the transforming function of E7.[35–37] The mutated E7 sequence was transferred to pNod.LucOAS by insertion between the 5′ restriction site NdeI and the 3′ site AgeI[38] (Figure S1). The pNod.LucOAS plasmid was kindly provided by Dr. Gelbart (UCLA).

Preparation of mRNA.

The pT7.Nod.E7OAS construct contained the T7 promoter and 5′ untranslated region (UTR), Nodamura replicon, HPV E7 (mutant) coding sequence, TMV OAS, and 3′ UTR (Figure S2). The plasmid was linearized with XbaI (Figure S3A) and purified using the QiaQuick PCR purification kit (Qiagen). *In vitro* transcription and capping were carried out using the HiScribe T7 ARCA mRNA Kit (New England Biolabs). The mRNA was then

purified by lithium chloride precipitation. The purity and quality of the transcribed mRNA were assessed by UV–vis spectroscopy, agarose gel electrophoresis, and evaluation using an Agilent 2100 bioanalyzer.

Characterization of Nod.HPVE7 mRNA.

Transfection.—Baby hamster kidney fibroblasts (BHK-21 cells) were seeded on coverslips in six-well plates containing Dulbecco's modified Eagle's complete medium supplemented with 10% fetal bovine serum (both from Thermo Fisher Scientific). The plates were incubated for 24 h at 37 °C in a 5% CO_2 incubator until they reached 70–90% confluency and were then transfected with 500 ng of Nod.HPV-E7 mRNA using Lipofectamine 2000 (Thermo Fisher Scientific) according to the manufacturer's instructions. The cells were incubated at 37 °C for 24–72 h as above, and gene expression was assessed by confocal imaging, real-time polymerase chain reaction (RT-PCR), and quantitative RT-PCR.

Confocal Microscopy.—Cells were fixed 24 h post-transfection in 4% (v/v) paraformaldehyde in phosphate-buffered saline (PBS) for 10 min at room temperature (RT) along with untransfected controls. The outer membrane was stained with wheat germ agglutinin (WGA) conjugated to Alexa Fluor 555 (Invitrogen; W32464), diluted to 1:1000. The cells were then permeabilized with 0.2% Triton X-100 (Sigma-Aldrich, X100) for 2 min and blocked with 10% (v/v) goat serum (Thermo Fisher Scientific, 16210064) in PBS for 1 h. HPV E7 protein was detected by staining the cells with an HPV 16 E7-specific polyclonal antibody (Invitrogen; PA5–117383), diluted to 1:50 in 5% (v/v) goat serum in PBS. Bound primary antibody was detected using a secondary goat antirabbit antibody conjugated to Alexa Fluor 647 (Invitrogen; A-21245), diluted to 1:500 in 5% (v/v) goat serum in PBS. The cells were washed 3 × 5 min in PBS between treatments. Finally, the cells were mounted using Fluoroshield containing 4′,6-diamidino-2-phenylindole (Sigma-Aldrich, F6057) and sealed under the coverslips with clear nail polish. Images were acquired using a Nikon A1R confocal microscope with a 60× oil immersion objective, and the image data were processed using Nikon NIS-Elements.

RT-PCR.—Total RNA was extracted from cells 24–72 h post-transfection with Nod.HPVE7 using the RNEasy Mini Kit (Qiagen). The isolated RNA was amplified by one-step RT-PCR using SuperScript IV reverse transcriptase (Thermo Fisher Scientific) and an E7-specific forward primer (5′-CAT ATG CAT GGA GAT ACA CCT-3′) and reverse primer (5′-CTA GAA CCG GTT TAT GGT TTC-3′). Reverse transcription was carried out for 10 min at 60 °C, and then cDNA was denatured at 98 °C for 2 min and amplified by applying 40 cycles of denaturation at 98 °C for 10 s/kb, annealing at 60 °C for 10 s/kb, and extending at 72 °C for 30 s/kb, with a final extension step at 72 °C for 5 min. The products were analyzed by 1% agarose gel electrophoresis in Tris-acetate-EDTA (1× TAE) buffer (pH 8.0; Fisher Scientific).

Quantitative RT-PCR.—RNA extracted 24–72 h post-transfection as described above was reverse transcribed using the RT2 first strand kit (Qiagen) and amplified using RT2SYBR Green qPCR Mastermix (Qiagen) and an E7-specific forward primer (5′-CGG ACA GAG

CCC ATT ACA ATA-3′) and reverse primer (5′-CTT CCA ACG TAC GGA TGT CTA C-3′) in a CFX96 real-time thermal cycler system (Bio-Rad). *GAPDH* cDNA was amplified for normalization, using a specific forward primer (5′-GAC TTC AAC AGT GAC TCC CAC-3′) and reverse primer (5′-TCT GTT GCT GTA GCC AAA TTC-3′). Mean CT values calculated using the $2^{-\Delta\Delta}$ CT method were used to determine the relative expression level of the E7 gene and the fold change in gene expression in the presence or absence of the Nodamura replicon. All experiments were carried out using triplicate samples.

Encapsulation of Nod.HPV.E7 mRNA in TMV-Like Particles.

TMV Coat Protein Preparation.—TMV was purified from infected *Nicotiana benthamiana* leaves as previously described[39] and 10 mg of TMV particles was mixed with two volumes of glacial acetic acid (Sigma-Aldrich; 34.8 M) for 20 min on ice, followed by centrifugation at 20000*g* for 20 min at 4 °C. The supernatant was collected and dialyzed against Milli-Q water for 48 h using a Spectra Por S/P 1 6–8 kDa dialysis membrane (Thermo Fisher Scientific). The precipitated coat protein was collected by centrifugation as above, and the pellet was resuspended in 75 mM sodium phosphate buffer (pH 7.2).

In Vitro Assembly of Nod.HPV.E7 mRNA with TMV Coat Protein.—Nod.HPV.E7 mRNA was allowed to self-assemble with TMV coat protein by mixing the two components at a 1:20 mRNA/protein mass ratio in sodium phosphate buffer (pH 7.2) and incubating at 30 °C for 16–18 h. The VLPs were treated with 50 μg of RNase A (Thermo Fisher Scientific) at 37 °C for 30 min and purified on a 100 kDa Amicon spin column.

Validation of Assembled TMV VLPs Encapsulating Nod.HPV.E7 mRNA.

UV–Vis Spectroscopy.—The concentration of TMV, coat protein, and assembled VLPs encapsulating Nod.HPV.E7 mRNA was measured by UV–vis spectroscopy using a Nanodrop 2000 device (Thermo Fisher Scientific). Beer's law was applied with the following extinction coefficients: TMV, $\varepsilon_{260\text{nm}} = 3\ \mu\text{L}\ \mu\text{g}^{-1}\ \text{cm}^{-1}$; TMV coat protein, $\varepsilon_{260\text{nm}} = 1.3\ \mu\text{L}\ \mu\text{g}^{-1}\ \text{cm}^{-1}$. The purity of TMV coat proteins confirmed by measuring the A_{260}/A_{280} and A_{280}/A_{250} absorbance ratios. The integrity of the VLPs was confirmed by comparing the A_{260}/A_{280} absorbance ratio to that of native TMV.

Size-Exclusion Chromatography (SEC).—The purity and integrity of assembled VLPs (0.2 mg/mL) were compared to native TMV and its coat protein using an ÄKTA pure fast protein liquid chromatography system equipped with a Superose 6 Increase column (GE Healthcare Life Sciences). The chromatography system was operated at a flow rate of 0.5 mL/min, with detectors fixed at 260 nm (nucleic acid) and 280 nm (protein).

Transmission Electron Microscopy (TEM).—Assembled VLPs (0.5 mg/mL) were visualized alongside native TMV and coat protein using a Tecnai G2 TF20 high-resolution electron microscope (FEI, Hillsboro). Formvar carbon-coated 300-mesh copper grids (Electron Microscopy Sciences) were rendered hydrophilic using the PELCO easiGlow operating system before negative staining with 2% (w/v) uranyl acetate (Agar Scientific), followed by imaging at 300 kV.

Immunization Studies.

Animal studies were conducted with the approval of the Institutional Animal Care and Use Committee (IACUC) of the University of California, San Diego. BALB/c female mice (n = 5; 6–7 weeks old) were obtained from the Jackson Laboratory, Bar Harbor, MA (strain #000651). Mice were immunized subcutaneously (s.c.) with 100 μg of TMV VLPs in PBS (pH 7.4; containing ~5 μg of Nod.HPVE7 mRNA encapsulated), following a prime (day 0) and boost (day 14) schedule. Dosing was selected based on previous reports using sa-mRNA vaccines for various antigens, as well as mRNA vaccines targeting HPV16 E6/E7.[40–44] In future studies, dose-range studies will be conducted. Blood was collected by retro-orbital bleeding before the prime (day 0) and then on days 14 and 28. Plasma was collected by centrifugation at 2000g for 10 min at 4 °C and stored at −20 °C.

Enzyme-Linked Immunosorbent Assay (ELISA).

The titers of E7-specific IgG in mouse serum on days 0, 14, and 28 were evaluated by ELISA. High-binding nickel-activated ELISA plates (Thermo Fisher Scientific) were coated overnight at 4 °C with 100 μL/well of His_6-tagged E7 protein (Genscript) at a concentration of 2 mg/mL in PBS (pH 7.4). The capture antisera were diluted to 1:100–1:2800 in PBS containing 2% bovine serum albumin (Sigma-Aldrich) and were incubated on a shaking platform at RT for 1 h. For detection, we added 100 μL/well of a goat antimouse secondary antibody (Thermo Fisher Scientific) conjugated to horseradish peroxidase (HRP), diluted to 1:5000 in PBS containing 0.05% Tween-20 (PBST), and incubated at RT for 1 h. After each incubation step, the plates were washed 3 × 5 min with 200 μL of PBST (pH 7.4). The signal was developed using a 100 μL/well 1-Step Ultra TMB-ELISA substrate solution (Thermo Fisher Scientific), active ingredient 3,3′,5,5′-tetramethylbenzidine, for 2 min at RT. The reaction was stopped with 50 μL of 1 M sulfuric acid (Spectrum Chemical). The absorbance was measured at 450 nm using an Infinite 200 Pro microplate reader. The reciprocal dilution at which the absorbance was twice that of the blank wells was calculated as the endpoint titer of the anti-E7 antisera.

Antibody Isotyping.

HPV16 E7-specific isotypes (IgG1, IgG2a, IgG2b, and IgM) in the antisera were determined using an ELISA protocol similar to that described above. The ELISA plate was coated as above, and the antisera were prepared and incubated as above. However, the detection step involved secondary antibodies specific for IgG1 (Invitrogen; PA174421), IgG2a (Thermo Fisher Scientific; A-10685), IgG2b (Abcam; ab97250), and IgM (Invitrogen; 31172), all diluted to 1:1000. The type of immune response was estimated from the IgG2a/IgG1 ratio.

In Vitro Splenocyte Proliferation Assay.

XTT Cell Proliferation Assay.—Spleens were harvested from vaccinated and PBS-injected mice on day 35. Splenocytes were prepared according to the Spleen Dissociation Kit, Mouse (Miltenyi Biotec), using a gentleMACS Octo Dissociator with Heaters. The collected cells were incubated with 1× RBC Lysis Buffer (Invitrogen) for 5 min at RT. Viable splenocytes were cultured in a 96-well plate (1×10^5 cells/well in 100 μL of medium), stimulated with 20 μg/mL of the HPV16 E7 protein or PBS (control), and then

incubated at 37 °C for 24, 48, and 72 h. Splenocyte proliferation was measured using the XTT Cell Proliferation Kit (Thermo Fisher Scientific). The culture supernatant was collected at different time points after stimulation to quantify interferon-gamma (IFN-γ) and interleukin-4 (IL-4) levels using cytokine-specific ELISA kits (BD Pharmingen).

ELISPOT Assay.—Splenocyte activation was also analyzed using a mouse double-color ELISPOT kit (Cellular Technology Limited). Briefly, the ELISPOT plate was coated overnight at 4 °C with capture antibody, antimouse IFN-γ and antimouse IL-4 antibodies (1:166). Spleens were harvested from Nod.HPV.E7 immunized and control mice on days 14 and 28. Splenocyte suspensions (5×10^6 cells/well) were stimulated with 100 μL of medium alone (negative control), HPV E7 (20 μg/mL), wild-type TMV (10 μg/mL) or 50 ng/mL phorbol 12-myristate 13-acetate (PMA), and 1 μg/mL ionomycin (both from Sigma-Aldrich) as a positive control, at 37 °C in a 5% CO_2 incubator for 24 h. After washing with PBST, the plates were incubated with FITC-labeled antimurine IFN-γ (1:1000 dilution) and biotin-labeled antimurine IL-4 (1:666) antibodies at RT for 2 h. The plates were washed, incubated with streptavidin–alkaline phosphatase (AP) (1:1000), and anti-FITC-HRP secondary antibodies (1:1000) at RT for 1 h, then washed again with PBST and distilled water, and incubated with AP substrate for 15 min and then with HRP substrate for 10 min at RT. The plates were then rinsed with water and air-dried at RT overnight before analysis with an S6 Entry M2 ELISpot reader (Cellular Technology Ltd.).

RESULTS AND DISCUSSION

Cloning, *In Vitro* Transcription, and Encapsulation of the E7 mRNA.

A mutated HPV16 E7 sequence (Figure S1) was inserted into the self-replicating Nod.HPVE7.OAS construct (Figure S2), and the linearized vector was used for *in vitro* transcription (Figure S3A). We confirmed the recovery of transcripts representing the Nod.HPVE7.OAS construct (4010 nt) and the E7 mRNA (303 nt) by electrophoresis (Figure S3B).

TMV was obtained from the infected leaves of *N. benthamiana* plants and the coat protein was isolated by glacial acetic acid disassembly. The TMV particles were rod-shaped with the typical native morphology as shown by TEM, and the absorbance ratios of A_{260}/A_{280} = 1.2 and A_{280}/A_{250} ~ 1 were as anticipated (Figure 1A, top panel). Disassembled coat proteins were also visualized by TEM, and the absorbance ratios of A_{260}/A_{280} ~ 0.65 and A_{280}/A_{250} ~ 2 indicated the coat protein was pure and devoid of viral genomic RNA (Figure 1A, middle panel). SEC showed typical elution profiles for the native TMV (~8 mL) and its coat proteins (~18 mL), confirming their integrity (Figure 1A, top and middle panels). The encapsulation of Nod.HPVE7.OAS mRNA *in vitro* at a protein/mRNA ratio of 20:1 allowed the assembly of VLPs ~ 188 nm in length, as confirmed by the high aspect ratio observed in TEM images, as well as A_{260}/A_{280} and A_{280}/A_{250} absorbance ratios and SEC profiles similar to native TMV particles (Figure 1A, bottom panel). The length of the packaged mRNA defines the length of TMV-based VLPs, and the predicted length of VLPs packaging Nod.HPVE7.OAS (4010 nt) was 188 nm. This was confirmed by TEM, which revealed VLPs with a mean length of 178.65 ± 17.03 nm. Total RNA was isolated from the VLPs and

amplified by RT-PCR using E7-specific primers, and the expected amplicon size of ~300 bp was confirmed by agarose gel electrophoresis (Figure 1B).

Expression of Replicons *In Vitro*.

BHK-21 cells were transfected with the Nod.HPVE7.OAS self-replicating construct, E7 mRNA, or with VLPs containing the Nod.HPVE7.OAS construct, and in all cases, we detected E7 mRNA and protein in the cells. One-step RT-PCR using E7-specific primers resulted in the amplification of a ~300-bp product from cell lysates, confirming that the VLP-mediated delivery of Nod.HPVE7.OAS into the cells was similar in efficiency to direct transfection with Nod.HPVE7.OAS RNA (Figure 2A). Quantitative RT-PCR showed a significant ~7-fold change in the abundance of E7 mRNA when delivered as the replicon versus the nonreplicon mRNA (***$p < 0.0001$ at 24 and 48 h and **$p = 0.0032$ at 72 h), and they both showed a significant (***$p < 0.0001$) increase compared to the nontransfected control (Figure 2B).

Kinetics and magnitude of antigen expression from self-amplifying mRNA have been reported in several animal models,[41,42,45] and our expression data aligns with these findings. We had previously shown a comparison kinetics of antigen expression from self-amplifying mRNA (sa-mRNA) to non-sa-mRNA using reporter genes such as renilla luciferase and fluorescent proteins.[46] At equal mRNA doses, expression from the sa-mRNA construct was initially lower due to the time required for replication of longer mRNA construct; important at the 24 h time point expression levels of the sa-mRNA construct significantly increased compared to mRNA alone, and this enhanced expression was pertinent over a 7-day time frame.[46] Overall this is consistent with the kinetic analysis performed over 3 days showing a significant fold change that decreases over time (***$p < 0.0001$ at 24 and 48 h and **$p = 0.0009$ at 72 h) (Figure 2B). Last, expression of HPVE7 protein was confirmed by confocal imaging (Figure 2C).

Immune Response to the VLP-Based mRNA Vaccine Candidate.

Mice were s.c. injected with VLPs using a primeboost regimen (immunization on days 0 and 14), and blood was collected on days 0, 14, and 28 (Figure 3A). The titer of E7-specific IgG increased significantly (***$p < 0.0001$ for dilutions of 1/100, 1/200, and 1/400) after the prime and boost immunizations (Figure 3B, left panel), with an endpoint titer of ~1:5120 (Figure 3B, right panel). Isotyping revealed high levels of E7-specific IgM and significant levels (***$p < 0.0001$) of IgG isotypes IgG1, IgG2a, and IgG2b (Figure 3C, left panel), confirming immunoglobulin class switching and differentiation. The high levels of IgM were expected because this is the first class of antibody expressed during B cell development in response to primary antigenic exposure.[47] The development of IgM antibodies against SARS-CoV-2 spike protein (S) following vaccination is associated with the development of a more effective humoral immune response, leading to long-lasting protection due to the production of anti-S IgG with higher affinity and neutralizing efficacy.[48,49] The IgG2a/IgG1 ratio was <1, indicating a Th2-biased immune response (Figure 3C, right panel).

Murine Splenocyte Proliferation *In Vitro* and E7-Specific T Cell Memory Response.

Vaccines should induce long-lived memory T cells that clonally expand and differentiate into effector cells when they encounter the previously administered antigen by producing IFN-γ, TNFα, and IL-2.[50,51] Spleen cell populations cultivated *in vitro* mature following stimulation with the E7 protein, causing naïve T cells to proliferate into E7-specific effector T cells. The elicitation of a T cell memory response following exposure to TMV.Nod.HPV-E7.OAS was evident from the increased proliferation of E7-stimulated splenocytes harvested from TMV.Nod.HPV-E7.OAS-immunized mice compared to PBS-immunized controls after 24 and 48 h (Figure 4A). Following stimulation, the proliferation index increased to ~1.76 after 24 h and ~1.5 after 48 h, as determined from the A_{450} stimulated/unstimulated absorbance ratio (Figure 4A).

The poststimulation culture supernatant showed significantly higher levels of IFN-γ (**p = 0.0073 at 24 h, ***p = 0.0003 at 48 h, and ***p = 0.0002 at 72 h) in the immunized mice (Figure 4B). ELISA revealed the presence of ~4303 pg/mL IFN-γ at 24 h, ~6058 pg/mL at 48 h, and ~6354 pg/mL at 72 h. ELISpot assays confirmed the significantly higher number of IFN-γ-secreting cells (***$p < 0.001$) among E7-stimulated splenocytes from the immunized mice (Figure 4B). Splenocyte proliferation and the generation of the Th1 signature cytokine IFN-γ, following the stimulation of splenocytes with E7, suggest priming of the T cell (memory) response in the vaccinated mice.

CONCLUSIONS

The FDA-approved HPV vaccines Gardasil, Gardasil 9, and Cervarix are effective as prophylactics but have no therapeutic efficacy following infection.[52] The development of therapeutic vaccines for individuals carrying oncogenic HPV16/18 strains has focused on DNA vaccines targeting the oncoproteins E6 and E7.[53] For example, a shuffled version of the HPV-16 E7 gene (HPV16 E7SH) elicited a cytotoxic T cell response, leading to tumor regression in a murine tumor model and the same gene was also effective *in vitro* following the transfection of human dendritic cells.[54] Similar DNA vaccines with shuffled and/or optimized E6 and E7 genes have been developed and tested in HPV16$^+$ mouse models, where they elicited potent E6/E7-specific cellular immune responses leading to tumor regression.[55] To increase immunogenicity and potency, shuffled oncogenes have been fused with plant genes, such as the maize γ-zein self-assembly domain known as Zera.[56] Other approaches include combinations with immunomodulators such as FLT3L and the anticancer monoclonal antibody pembrolizumab.[57] Although there has been some progress in clinical development, no therapeutic vaccines are currently approved for human use.[58]

The rapid development of mRNA vaccines in response to COVID-19 has generated interest in the application of this technology against HPV. The efficacy of an LNP-encapsulated mRNA vaccine encoding HPV E7 (HPV mRNA-LNP) was demonstrated in a mouse model of HPV$^+$ oropharyngeal squamous cell carcinoma.[43] As an alternative to LNPs, we tested VLPs derived from the plant virus TMV because plant viruses have inherent immunostimulatory properties, acting as an adjuvant as well as a carrier.[59] We demonstrated the suitability of TMV as a platform for the development of therapeutic HPV vaccines by

using it to deliver a self-amplifying shuffled E7 mRNA, which elicited a potent humoral and cellular immune response in mice.

Our work lays the foundation for the development of TMV-based therapeutic vaccines against HPV and can be expanded to include combinations of E6 and E7 to trigger a more potent and durable immune response. Future work should compare the benefits of VLPs and LNPs in terms of efficacy, safety, stability, and manufacturing efficiency. HPV^+ cancers disproportionately affect people in low- and middle-income countries, and the limited access to HPV vaccines, screening programs, and treatment options contributes to this disparity.[60] The proposed TMV technology may be particularly suitable to address health inequality issues because molecular farming protocols can be established in the region for the region, exploiting the ability to produce TMV without sophisticated equipment and infrastructure or a cold chain, thus also reducing the costs of distribution.[22] TMV is suitable as a VLP platform for the delivery of mRNA vaccines and can preserve their integrity and functionality *in vitro* and *in vivo*, providing a new therapeutic strategy against HPV and other viruses.

Supplementary Material

Refer to Web version on PubMed Central for supplementary material.

ACKNOWLEDGMENTS

The authors thank the University of California, San Diego, Cellular and Molecular Medicine Electron Microscopy Core (UCSD-CMM-EM Core; RRID SCR_022039) for equipment access and technical assistance. The UCSD-CMM-EM Core is partly supported by NIH Award S10OD023527. The authors thank the Kersi Pestonjamasp and UCSD Cancer Center Microscopy Shared Facility (Specialized Support Grants P30 CA23100-28 and 2P30CA023100 by NCI) for providing equipment, services, and expertise to complete this work.

Funding

This work was supported in part by NIH Grants R21 AI161306, R01 CA224605, R01 CA253615 (including CA253615-2S1) and NSF Award CBET-2134535.

Data Availability Statement

Data will be made available from the author upon reasonable request.

REFERENCES

(1). Verbeke R; Lentacker I; De Smedt SC; Dewitte H Three decades of messenger RNA vaccine development. Nano Today 2019, 28, 100766.

(2). Park KS; Sun X; Aikins ME; Moon JJ Non-viral COVID-19 vaccine delivery systems. Adv. Drug Deliv Rev 2021, 169, 137–151. [PubMed: 33340620]

(3). Zhang G; Tang T; Chen Y; Huang X; Liang T mRNA vaccines in disease prevention and treatment. Signal Transduct Target Ther 2023, 8 (1), 365. [PubMed: 37726283]

(4). Li Y; Wang M; Peng X; Yang Y; Chen Q; Liu J; She Q; Tan J; Lou C; Liao Z; et al. mRNA vaccine in cancer therapy: Current advance and future outlook. Clin Transl Med 2023, 13 (8), No. e1384.

(5). Barbier AJ; Jiang AY; Zhang P; Wooster R; Anderson DG The clinical progress of mRNA vaccines and immunotherapies. Nat. Biotechnol 2022, 40 (6), 840–854. [PubMed: 35534554]

(6). Gote V; Bolla PK; Kommineni N; Butreddy A; Nukala PK; Palakurthi SS; Khan W A Comprehensive Review of mRNA Vaccines. Int. J. Mol. Sci 2023, 24 (3), 2700. [PubMed: 36769023]

(7). Pardi N; Hogan MJ; Porter FW; Weissman D mRNA vaccines - a new era in vaccinology. Nat. Rev. Drug Discov 2018, 17 (4), 261–279. [PubMed: 29326426]

(8). Kowalski PS; Rudra A; Miao L; Anderson DG Delivering the Messenger: Advances in Technologies for Therapeutic mRNA Delivery. Mol. Ther 2019, 27 (4), 710–728. [PubMed: 30846391]

(9). Mohsen MO; Augusto G; Bachmann MF The 3Ds in virus-like particle based-vaccines: ″Design, Delivery and Dynamics″. Immunol Rev 2020, 296 (1), 155–168. [PubMed: 32472710]

(10). Zhou Y; Maharaj PD; Mallajosyula JK; McCormick AA; Kearney CM In planta production of flock house virus transencapsidated RNA and its potential use as a vaccine. Mol. Biotechnol 2015, 57 (4), 325–336. [PubMed: 25432792]

(11). Biddlecome A; Habte HH; McGrath KM; Sambanthamoorthy S; Wurm M; Sykora MM; Knobler CM; Lorenz IC; Lasaro M; Elbers K; et al. Delivery of self-amplifying RNA vaccines in in vitro reconstituted virus-like particles. PLoS One 2019, 14 (6), No. e0215031.

(12). Wege C; Koch C From stars to stripes: RNA-directed shaping of plant viral protein templates-structural synthetic virology for smart biohybrid nanostructures. Wiley Interdiscip Rev. Nanomed Nanobiotechnol 2020, 12 (2), No. e1591.

(13). Lomonossoff GP; Wege C TMV Particles: The Journey From Fundamental Studies to Bionanotechnology Applications. Adv. Virus Res 2018, 102, 149–176. [PubMed: 30266172]

(14). Sleat DE; Turner PC; Finch JT; Butler PJ; Wilson TM Packaging of recombinant RNA molecules into pseudovirus particles directed by the origin-of-assembly sequence from tobacco mosaic virus RNA. Virology 1986, 155 (2), 299–308. [PubMed: 18640655]

(15). Maharaj PD; Mallajosyula JK; Lee G; Thi P; Zhou Y; Kearney CM; McCormick AA Nanoparticle encapsidation of Flock house virus by auto assembly of Tobacco mosaic virus coat protein. Int. J. Mol. Sci 2014, 15 (10), 18540–18556. [PubMed: 25318056]

(16). Smith ML; Corbo T; Bernales J; Lindbo JA; Pogue GP; Palmer KE; McCormick AA Assembly of trans-encapsidated recombinant viral vectors engineered from Tobacco mosaic virus and Semliki Forest virus and their evaluation as immunogens. Virology 2007, 358 (2), 321–333. [PubMed: 17014881]

(17). Lam P; Steinmetz NF Plant viral and bacteriophage delivery of nucleic acid therapeutics. Wiley Interdiscip Rev. Nanomed. Nanobiotechnol 2018, 10 (1). DOI: 10.1002/wnan.1487.

(18). Gallie DR; Sleat DE; Watts JW; Turner PC; Wilson TM In vivo uncoating and efficient expression of foreign mRNAs packaged in TMV-like particles. Science 1987, 236 (4805), 1122–1124. [PubMed: 3472350]

(19). Shukla S; Hu H; Cai H; Chan SK; Boone CE; Beiss V; Chariou PL; Steinmetz NF Plant Viruses and Bacteriophage-Based Reagents for Diagnosis and Therapy. Annu. Rev. Virol 2020, 7 (1), 559–587. [PubMed: 32991265]

(20). Wouters OJ; Shadlen KC; Salcher-Konrad M; Pollard AJ; Larson HJ; Teerawattananon Y; Jit M Challenges in ensuring global access to COVID-19 vaccines: production, affordability, allocation, and deployment. Lancet 2021, 397 (10278), 1023–1034. [PubMed: 33587887]

(21). Zahmanova G; Aljabali AA; Takova K; Toneva V; Tambuwala MM; Andonov AP; Lukov GL; Minkov I The Plant Viruses and Molecular Farming: How Beneficial They Might Be for Human and Animal Health? Int. J. Mol. Sci 2023, 24 (2), 1533. [PubMed: 36675043]

(22). Rybicki EP Plant molecular farming of virus-like nanoparticles as vaccines and reagents. Wiley Interdiscip Rev. Nanomed Nanobiotechnol 2020, 12 (2), No. e1587.

(23). Kemnade JO; Seethammagari M; Collinson-Pautz M; Kaur H; Spencer DM; McCormick AA Tobacco mosaic virus efficiently targets DC uptake, activation and antigen-specific T cell responses in vivo. Vaccine 2014, 32 (33), 4228–4233. [PubMed: 24923637]

(24). Bachmann MF; Jennings GT Vaccine delivery: a matter of size, geometry, kinetics and molecular patterns. Nat. Rev. Immunol 2010, 10 (11), 787–796. [PubMed: 20948547]

(25). Albakri MM; Veliz FA; Fiering SN; Steinmetz NF; Sieg SF Endosomal toll-like receptors play a key role in activation of primary human monocytes by cowpea mosaic virus. Immunology 2020, 159 (2), 183–192. [PubMed: 31630392]

(26). Carignan D; Herblot S; Laliberte-Gagne ME; Bolduc M; Duval M; Savard P; Leclerc D Activation of innate immunity in primary human cells using a plant virus derived nanoparticle TLR7/8 agonist. Nanomedicine 2018, 14 (7), 2317–2327. [PubMed: 29128662]

(27). George P; Mani S; Abraham P; Michael RC The Association of Human Papillomavirus in Benign and Malignant Laryngeal Lesions-a Pilot Study. Indian J. Surg Oncol 2021, 12 (2), 306–310.

(28). Gheit T Mucosal and Cutaneous Human Papillomavirus Infections and Cancer Biology. Front Oncol 2019, 9, 355. [PubMed: 31134154]

(29). Yu L; Majerciak V; Zheng ZM HPV16 and HPV18 Genome Structure, Expression, and Post-Transcriptional Regulation. Int. J. Mol. Sci 2022, 23 (9), 4943. [PubMed: 35563334]

(30). Yu L; Majerciak V; Zheng ZM HPV16 and HPV18 Genome Structure, Expression, and Post-Transcriptional Regulation. Int. J. Mol. Sci 2022, 23 (9), 4943. [PubMed: 35563334]

(31). Yim EK; Park JS The role of HPV E6 and E7 oncoproteins in HPV-associated cervical carcinogenesis. Cancer Res. Treat 2005, 37 (6), 319–324. [PubMed: 19956366]

(32). Pal A; Kundu R Human Papillomavirus E6 and E7: The Cervical Cancer Hallmarks and Targets for Therapy. Front Microbiol 2020, 10, 3116. [PubMed: 32038557]

(33). Vats A; Trejo-Cerro O; Thomas M; Banks L Human papillomavirus E6 and E7: What remains? Tumour Virus Res 2021, 11, 200213. [PubMed: 33716206]

(34). Zanier K; ould M'hamed ould Sidi A; Boulade-Ladame C; Rybin V; Chappelle A; Atkinson A; Kieffer B; Trave G Solution structure analysis of the HPV16 E6 oncoprotein reveals a self-association mechanism required for E6-mediated degradation of p53. Structure 2012, 20 (4), 604–617. [PubMed: 22483108]

(35). Patrick DR; Zhang K; Defeo-Jones D; Vuocolo GR; Maigetter RZ; Sardana MK; Oliff A; Heimbrook DC Characterization of functional HPV-16 E7 protein produced in Escherichia coli. J. Biol. Chem 1992, 267 (10), 6910–6915. [PubMed: 1551900]

(36). Smahel M; Sima P; Ludvikova V; Vonka V Modified HPV16 E7 Genes as DNA Vaccine against E7-Containing Oncogenic Cells. Virology 2001, 281 (2), 231–238. [PubMed: 11277695]

(37). Peng S; Ferrall L; Gaillard S; Wang C; Chi WY; Huang CH; Roden RBS; Wu TC; Chang YN; Hung CF Development of DNA Vaccine Targeting E6 and E7 Proteins of Human Papillomavirus 16 (HPV16) and HPV18 for Immunotherapy in Combination with Recombinant Vaccinia Boost and PD-1 Antibody. mBio 2021, 12 (1), 1–19.

(38). Gitlin L; Hagai T; LaBarbera A; Solovey M; Andino R Rapid evolution of virus sequences in intrinsically disordered protein regions. PLoS Pathog 2014, 10 (12), No. e1004529.

(39). Chan SK; Steinmetz NF Isolation of Tobacco Mosaic Virus-Binding Peptides for Biotechnology Applications. Chembiochem 2022, 23 (11), No. e202200040.

(40). Magini D; Giovani C; Mangiavacchi S; Maccari S; Cecchi R; Ulmer JB; De Gregorio E; Geall AJ; Brazzoli M; Bertholet S Self-Amplifying mRNA Vaccines Expressing Multiple Conserved Influenza Antigens Confer Protection against Homologous and Heterosubtypic Viral Challenge. PLoS One 2016, 11 (8), No. e0161193.

(41). Maruggi G; Mallett CP; Westerbeck JW; Chen T; Lofano G; Friedrich K; Qu L; Sun JT; McAuliffe J; Kanitkar A; et al. A self-amplifying mRNA SARS-CoV-2 vaccine candidate induces safe and robust protective immunity in preclinical models. Mol. Ther 2022, 30 (5), 1897–1912. [PubMed: 34990810]

(42). Pepini T; Pulichino AM; Carsillo T; Carlson AL; Sari-Sarraf F; Ramsauer K; Debasitis JC; Maruggi G; Otten GR; Geall AJ; et al. Induction of an IFN-Mediated Antiviral Response by a Self-Amplifying RNA Vaccine: Implications for Vaccine Design. J. Immunol 2017, 198 (10), 4012–4024. [PubMed: 28416600]

(43). Qiu K; Duan X; Mao M; Song Y; Rao Y; Cheng D; Feng L; Shao X; Jiang C; Huang H; et al. mRNA-LNP vaccination-based immunotherapy augments CD8(+) T cell responses against HPV-positive oropharyngeal cancer. NPJ. Vaccines 2023, 8 (1), 144. [PubMed: 37773254]

(44). Zhou K; Yuzhakov O; Behloul N; Wang D; Bhagat L; Chu D; Zhang X; Cheng X; Fan L; Huang X; et al. HPV16 E6/E7 -based mRNA vaccine is therapeutic in mice bearing aggressive HPV-positive lesions. Front Immunol 2023, 14, 1213285. [PubMed: 37503351]

(45). Vogel AB; Lambert L; Kinnear E; Busse D; Erbar S; Reuter KC; Wicke L; Perkovic M; Beissert T; Haas H; et al. Self-Amplifying RNA Vaccines Give Equivalent Protection against Influenza to mRNA Vaccines but at Much Lower Doses. Mol. Ther 2018, 26 (2), 446–455. [PubMed: 29275847]

(46). Karan S; Duran-Meza AL; Chapman A; Tanimoto C; Chan SK; Knobler CM; Gelbart WM; Steinmetz NF In Vivo Delivery of Spherical and Cylindrical In Vitro Reconstituted Virus-like Particles Containing the Same Self-Amplifying mRNA. Mol. Pharmaceutics 2024, 21 (6), 2727–2739.

(47). Gong S; Ruprecht RM Immunoglobulin M: An Ancient Antiviral Weapon - Rediscovered. Front Immunol 2020, 11, 1943. [PubMed: 32849652]

(48). Piubelli C; Ruggiero A; Calciano L; Mazzi C; Castilletti C; Tiberti N; Caldrer S; Verze M; Longoni SS; Accordini S; et al. Subjects who developed SARS-CoV-2 specific IgM after vaccination show a longer humoral immunity and a lower frequency of infection. EBioMedicine 2023, 89, 104471. [PubMed: 36796232]

(49). Ruggiero A; Piubelli C; Calciano L; Accordini S; Valenti MT; Carbonare LD; Siracusano G; Temperton N; Tiberti N; Longoni SS; et al. SARS-CoV-2 vaccination elicits unconventional IgM specific responses in naive and previously COVID-19-infected individuals. EBioMedicine 2022, 77, 103888. [PubMed: 35196644]

(50). Seder RA; Darrah PA; Roederer M T-cell quality in memory and protection: implications for vaccine design. Nat. Rev. Immunol 2008, 8 (4), 247–258. [PubMed: 18323851]

(51). Darrah PA; Patel DT; De Luca PM; Lindsay RW; Davey DF; Flynn BJ; Hoff ST; Andersen P; Reed SG; Morris SL; et al. Multifunctional TH1 cells define a correlate of vaccine-mediated protection against Leishmania major. Nat. Med 2007, 13 (7), 843–850. [PubMed: 17558415]

(52). Mo Y; Ma J; Zhang H; Shen J; Chen J; Hong J; Xu Y; Qian C Prophylactic and Therapeutic HPV Vaccines: Current Scenario and Perspectives. Front Cell Infect Microbiol 2022, 12, 909223. [PubMed: 35860379]

(53). Devaraja K; Aggarwal S; Singh M Therapeutic Vaccination in Head and Neck Squamous Cell Carcinoma-A Review. Vaccines (Basel) 2023, 11 (3), 634. [PubMed: 36992219]

(54). Ohlschlager P; Pes M; Osen W; Durst M; Schneider A; Gissmann L; Kaufmann AM An improved rearranged Human Papillomavirus Type 16 E7 DNA vaccine candidate (HPV-16 E7SH) induces an E7 wildtype-specific T cell response. Vaccine 2006, 24 (15), 2880–2893. [PubMed: 16472545]

(55). Almajhdi FN; Senger T; Amer HM; Gissmann L; Ohlschlager P Design of a highly effective therapeutic HPV16 E6/E7-specific DNA vaccine: optimization by different ways of sequence rearrangements (shuffling). PLoS One 2014, 9 (11), No. e113461.

(56). Whitehead M; Ohlschlager P; Almajhdi FN; Alloza L; Marzabal P; Meyers AE; Hitzeroth II; Rybicki EP Human papillomavirus (HPV) type 16 E7 protein bodies cause tumour regression in mice. BMC Cancer 2014, 14, 367. [PubMed: 24885328]

(57). Youn JW; Hur SY; Woo JW; Kim YM; Lim MC; Park SY; Seo SS; No JH; Kim BG; Lee JK; et al. Pembrolizumab plus GX-188E therapeutic DNA vaccine in patients with HPV-16-positive or HPV-18-positive advanced cervical cancer: interim results of a single-arm, phase 2 trial. Lancet Oncol 2020, 21 (12), 1653–1660. [PubMed: 33271094]

(58). Yan F; Cowell LG; Tomkies A; Day AT Therapeutic Vaccination for HPV-Mediated Cancers. Curr. Otorhinolaryngol Rep 2023, 11 (1), 44–61. [PubMed: 36743978]

(59). Murray AA; Wang C; Fiering S; Steinmetz NF In Situ Vaccination with Cowpea vs Tobacco Mosaic Virus against Melanoma. Mol. Pharmaceutics 2018, 15 (9), 3700–3716.

(60). Casas CPR; Albuquerque RCR; Loureiro RB; Gollner AM; Freitas MG; Duque G; Viscondi JYK Cervical cancer screening in low- and middle-income countries: A systematic review of economic evaluation studies. Clinics (Sao Paulo) 2022, 77, 100080. [PubMed: 35905574]

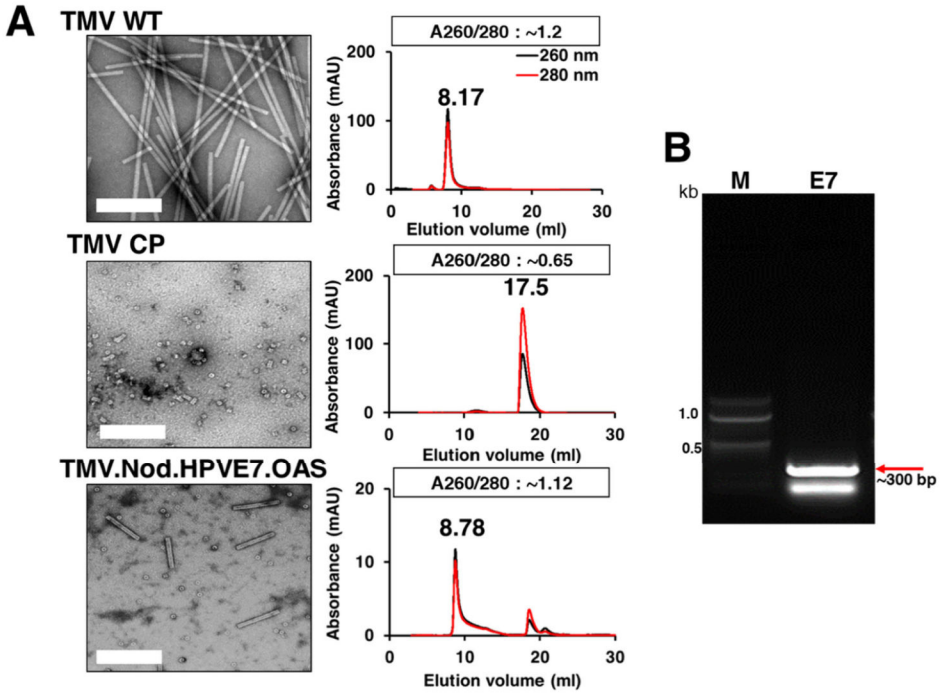

Figure 1.

Characterization of TMV.Nod.HPVE7.OAS VLPs. (A) TEM images of negatively stained VLPs and size-exclusion elution profiles of VLPs (black and red lines indicate 260 and 280 nm, respectively). Top panel = native TMV; middle panel = coat proteins; bottom panel = reassembled TMV.Nod.HPVE7.OAS VLPs. (B) Encapsulation of Nod.HPVE7.OAS mRNA into TMV confirmed by isolating RNA from assembled VLPs for RT-PCR analysis. The arrow indicates the HPV E7 amplicon (anticipated size ~300 bp). The lower-molecular-weight band is likely to be a primer dimer.

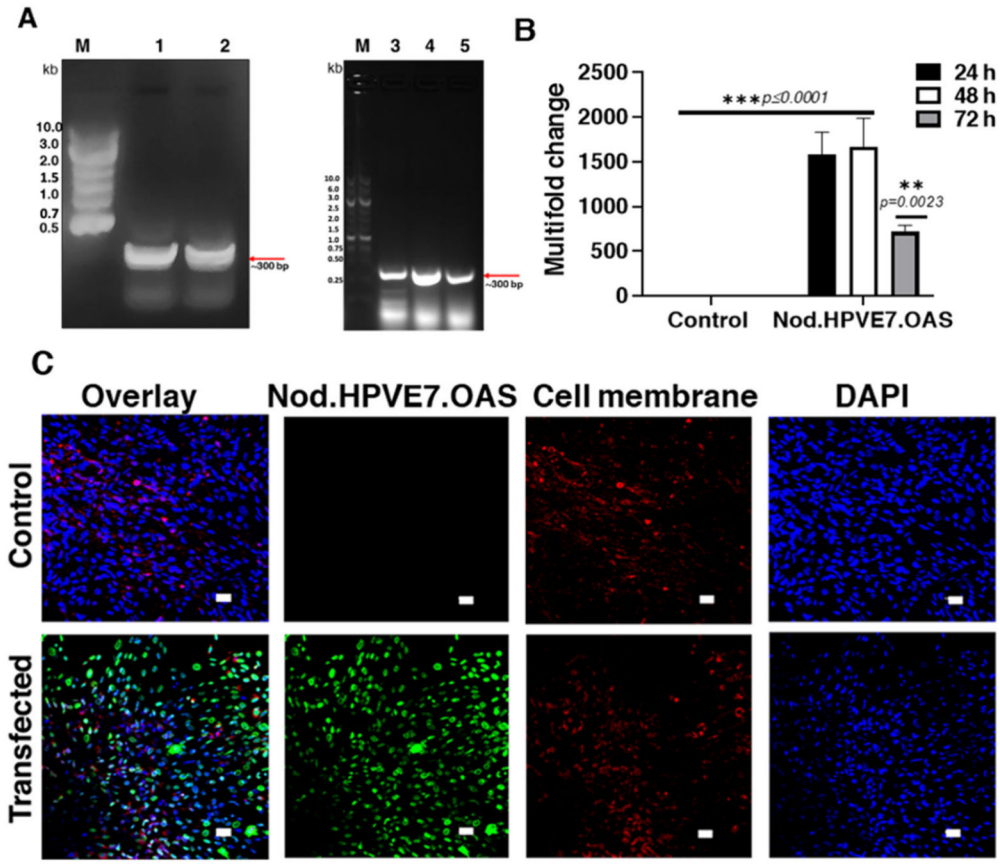

Figure 2.

Expression of E7 mRNA and protein using the Nod.HPVE7.OAS construct delivered directly as mRNA or packaged in VLPs. (A) Transfection of BHK-21 cells with Nod.HPVE7.OAS (lane 1), HPV E7 mRNA (lane 2) (500 ng/well), or exposure to TMV.Nod.HPVE7.OAS mRNA encapsulated in VLPs (lanes 3–5, 10, 20, and 40 μg of VLPs containing ~500 ng, ~1 μg, and 2 μg of Nod.HPVE7.OAS mRNA, respectively). Total RNA was isolated from cell lysates after 24 h and analyzed by RT-PCR. The anticipated size of the E7 amplicon was ~300 bp, as confirmed by 1% (w/v) agarose gel electrophoresis. (B) Analysis of transcript levels by quantitative RT-PCR and multifold change relative to HPV E7 mRNA based on RNA collected from BHK-21 cells transfected with Nod.HPVE7.OAS or HPV E7 mRNA (500 ng/well). HPV E7 expression was normalized to the reference gene *GAPDH*. Data are mean ± standard errors ($n = 3$). The statistical significance of multifold and relative multifold changes was determined by two-way ANOVA using Tukey's multiple comparisons test compared to control cells and the presence of the replicon. (C) Immunofluorescence imaging of BHK-21 cells (blue channel showing the nucleus staining and cell membrane staining by WGA in the red channel) transfected with Nod.HPVE7.OAS mRNA to confirm the presence of E7 protein (green channel; anti-HPV 16 E7 conjugated to Alexa Fluor 647). Scale bar = 10 μm.

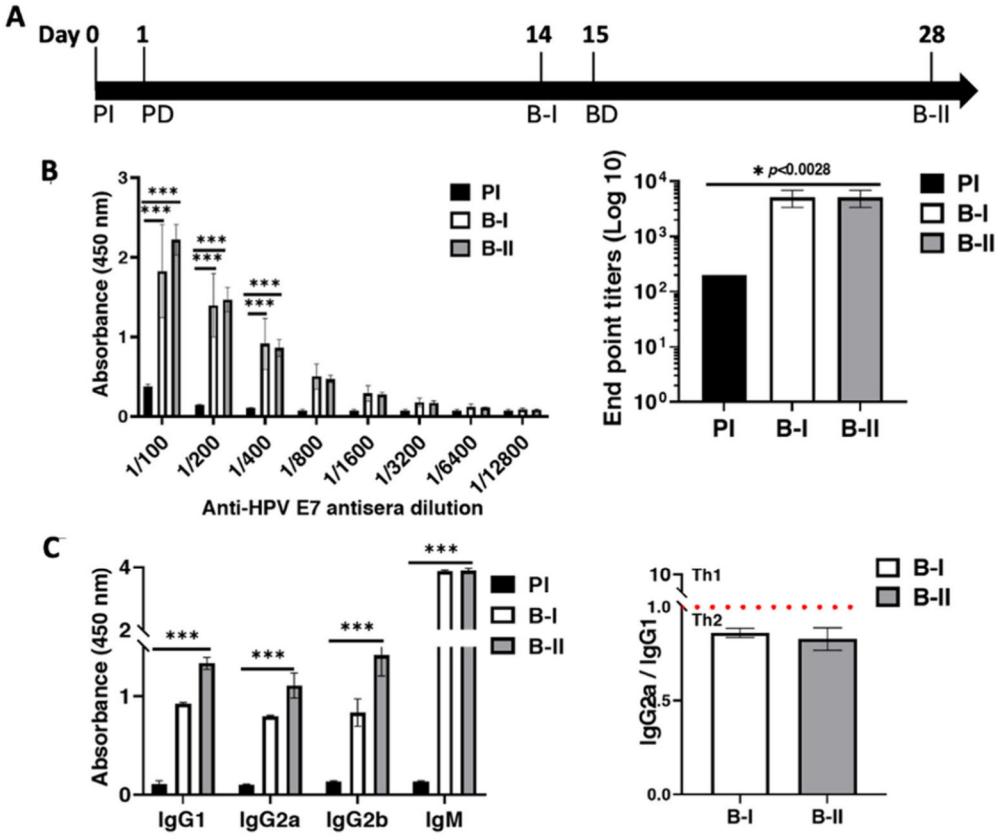

Figure 3.

Immunogenicity of the TMV.Nod.HPVE7.OAS mRNA vaccine. (A) BALB/c mice were immunized s.c. following a prime (PD, prime dose)–boost (BD, booster dose) schedule with 100 μg of VLPs on days 1 and 14. Antisera were collected by retro-orbital bleeding on days 0 (PI, preimmune sera), 14 (B-I, Bleed-I), and 28 (B-II, Bleed-II). (B) E7-specific IgG antibody titer antibodies analyzed by ELISA. Data are mean ± standard errors (n = 5 per group). Statistical significance was determined by two-way ANOVA with Tukey's multiple comparisons test (***$p < 0.0001$). (C) The isotype profile (IgG1, IgG2a, IgG2b and IgM) suggested a Th2-biased immune response to the VLP-based mRNA vaccine candidate. Data are mean ± standard errors (n = 5 per group). Statistical significance was determined by one-way ANOVA followed by Tukey's multiple comparisons test.

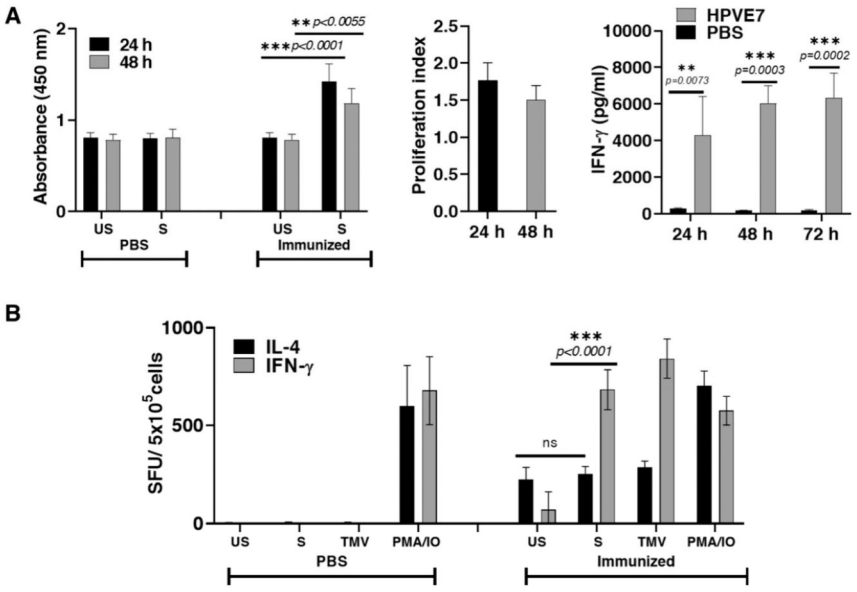

Figure 4.

Splenocyte proliferation response to HPV E7. (A) Proliferation of splenocytes isolated from TMV.Nod.HPVE7.OAS or PBS-immunized mice and stimulated with HPV16 E7 protein (20 μg/mL) or PBS (control) for 24 and 48 h. Splenocyte proliferation was measured using an XTT cell proliferation assay. The poststimulation culture supernatant collected at different time points was tested for the presence of IFN-γ and IL-4 using cytokine-specific ELISA kits. Data are mean ± standard errors (n = 3). Statistical significance was determined by two-way ANOVA with Tukey's multiple comparisons test. (B) ELISpot responses in splenocytes isolated from mice vaccinated with TMV.Nod.HPVE7.OAS or PBS and stimulated (S) with 20 μg/mL HPV E7, 10 μg/mL native TMV, or 50 ng/mL phorbol 12-myristate 13-acetate +1 μg/mL ionomycin (PMA/IO) as a positive control, along with unstimulated (US) or PBS-stimulated negative controls. Spot-forming units per 5×10^6 cells (SFU) were quantified for cytokines IL-4 and IFN-γ. Data are mean ± standard errors (n = 3, HPV E7 immunized group; n = 1, control group). Statistical significance was determined by two-way ANOVA with Tukey's multiple comparisons test.